# FRACTURE OF HIGH-STRENGTH CONCRETE:
## Implications for Structural Applications

**By David Darwin**[1]

**ABSTRACT:** Structural properties of reinforced concrete, such as bond and shear strength, that depend on the tensile properties of concrete are much lower for high-strength concrete than would be expected based on relationships developed for normal-strength concretes. To determine the reason for this behavior, studies at the University of Kansas have addressed the effects of aggregate type, water-cementitious material ratio, and age on the mechanical and fracture properties of normal and high-strength concretes. The relationships between compressive strength, flexural strength, and fracture properties were studied. At the time of test, concrete ranged in age from 5 to 180 days. Water-cementitious material ratios ranged from 0.24 to 0.50, producing compressive strengths between 20 MPa (2,920 psi) and 99 MPa (14,320 psi). Mixes contained either basalt or crushed limestone aggregate, with maximum sizes of 12 mm ($^1/_2$ in.) or 19 mm ($^3/_4$ in.). The tests demonstrate that the higher quality basalt coarse aggregate provides higher strengths in compression than limestone only for the high-strength concrete, but measurably higher strengths in flexure, and significantly higher fracture energies than the limestone coarse aggregate at all water-cementitious material ratios and ages. Compressive strength, water-cementitious material ratio, and age have no apparent relationship with fracture energy, which is principally governed by coarse aggregate properties. The peak bending stress in the fracture test is linearly related to flexural strength. Overall, as concrete strength increases, the amount of energy stored in the material at the peak tensile load increases, but the ability of the material to dissipate energy remains nearly constant. This suggests that, as higher strength cementitious materials are placed in service, the probability of nonductile failures will measurably increase. Both research and educational effort will be needed to develop strategies to limit the probability of brittle failures and inform the design community of the nature of the problems associated with high-strength concrete.

---

[1] Deane E. Ackers Distinguished Professor of Civil Engineering and Director of the Infrastructure Research Institute and the Structural Engineering and Materials Laboratory, University of Kansas, Lawrence, Kansas 66045, USA. email: daved@ukans.edu

## INTRODUCTION

High-strength concrete is a material that is used principally for its increased compressive strength and, for many years, its principal application was in lower-story columns of high-rise buildings. Although high-strength concrete represents only a small fraction of total concrete production, it allows major reductions in column cross-sections, thereby providing more usable floor area. For this reason, the use of high-strength concrete has been critical to the selection of framing systems that would have otherwise been structural steel. Over the years, high-strength concrete has seen broader applications, such as in building shear and bearing walls and bridge girders, especially for long-span bridges, where the flange thickness depends on the concrete compressive strength. These more recent applications, however, involve more than the compressive strength of the material. Of particular interest are loading cases, such as bond between reinforcing steel and concrete and shear strength, in which the tensile strength of concrete plays an important role. Typically, design procedures for bond and shear assign a strength that is proportional to the square root of the compressive strength $\sqrt{f_c'}$ (ACI 318-99). Research, however, has demonstrated that bond and shear strength in reinforced concrete increase more slowly than $\sqrt{f_c'}$ as the compressive strength of concrete increases above about 55 MPa (8000 psi). The principal goal of this paper is to establish the reason for this lower rate of strength gain.

## BACKGROUND

Research at the University of Kansas and at the University of Toronto amply illustrates the reduced effectiveness of high-strength concrete under tensile loading.

### Bond

In long-term studies at the University of Kansas to improve the bond strength between reinforcing steel and concrete (Darwin et al. 1992, 1993, 1996a, 1996b, 1998, Tholen and Darwin 1998, Zuo and Darwin 2000), it has been clearly established that the bond strength of



12 2000년도 가을 학술발표회 논문집

reinforcing bars that are not confined by transverse reinforcement increases more slowly than $\sqrt{f_c'}$. Using the results of splice specimens of the type illustrated in Figure 1, with compressive strength ranging from 18 to 108 MPa (2,610 to 15,650 psi), a best-fit equation using $\sqrt{f_c'}$ to characterize the concrete contribution to bond strength results in a reasonably accurate expression, but one that consistently underestimates the bond strength of specimens cast with low-strength concrete and overestimates the bond strength of specimens cast with high-strength concrete, as shown in Figure 2. Using the same test results, but optimizing the results to determine the best power of $f_c'$ provides a better match with the test data and a prediction with an accuracy that is independent of concrete strength, as shown in Figure 3. Based on that analysis, $f_c'^{1/4}$ is shown to best represent the concrete contribution to bond strength. This is in spite of the fact that data clearly shows that the tensile strength of concrete increases with at least the one-half power of the compressive strength of concrete (Ahmad and Shah 1985, Kozul and Darwin 1997, Barham and Darwin 1999). Also of interest are the experimental observations that members cast with higher strength aggregates exhibit higher bond strengths than members cast with lower strength aggregates and that the addition of transverse reinforcement provides a sizable incremental increase in bond strength (Darwin et al. 1996b, Zuo and Darwin 1998, 2000).

In conjunction with the experimental work, finite element analyses of bond specimens indicate that fracture mechanics models provide an excellent representation of actual behavior (Brown et al. 1993, Tholen and Darwin 1996). Finite element models of the beam-end bond specimen (Figures 4a and 4b) produce results, shown in Figures 5 and 6, that closely match experimental behavior, including an increasing maximum bond force with (1) increasing concrete cover and development length (Figure 5) and (2) an increasing product of the development length and the cover to the center of the bar (Figure 6). The key observation, in the results illustrated in Figures 5 and 6, is that a fracture mechanics model can provide an accurate representation of bond behavior. Thus, an understanding of the fracture behavior of concrete will provide an improved understanding of bond test results.

**Shear Strength**

In work at the University of Toronto, Collins and Kuchma (1999) studied the shear strength of lightly reinforced full-scale reinforced concrete beams as a function of compressive strength (Figure 7). In design, shear strength, also referred to as diagonal tension strength, is usually represented as an increasing function of $\sqrt{f_c'}$. In the study, concrete compressive strength ranged from 36 to 99 MPa (5,700 to 14,400 psi). In general, Collins and Kuchma observed no increase in shear strength for values of compressive strength above 50 MPa (7,250 psi) and, in fact, observed an 18% absolute drop in shear strength for a pair of 1 m (39.4 in.) deep beams without stirrups as the compressive strength increased from 36 MPa (5700 psi) to 99 MPa (14,440 psi). A small amount of transverse reinforcement in a third beam allowed the high-strength concrete member to more than meet its design shear strength.

Like the work on bond, the work at the University of Toronto clearly demonstrates that some aspect of concrete tensile behavior other than tensile strength plays a key role in the performance of high-strength concrete members in cases where tensile behavior governs member strength. As demonstrated next, a look at the total fracture behavior of concrete shows what that aspect is.

## FRACTURE STUDIES

Two studies at the University of Kansas (Kozul and Darwin 1997, Barham and Darwin 1999) were specifically designed to compare the performance of normal and high-strength concretes under tensile loading. A key goal in both studies was to better understand the observed behavior of structural members subjected to loading regimes governed by the tensile behavior of concrete. The studies consisted of the fabrication and testing of compression, flexure, and fracture specimens for concretes covering a broad range of compressive strengths and constituent material properties.

The studies involved concretes with water-cementitious material ratios (*w/cm*) ranging between 0.24 and 0.5, producing compressive strengths between 20 and 99 MPa (2920 and 14,320 psi). The mixes contained either crushed limestone or basalt aggregate with maximum sizes of 12 mm (1/2 in.) or 19 mm (3/4 mm). Of particular interest, was the difference in the aggregate properties, with the limestone possessing a compressive strength of 100 MPa (15,000 psi) and modulus of elasticity of 35 GPa (5,000,000 psi), while the basalt had a compressive strength of 340 MPa (50,000 psi) and a modulus of elasticity of 69 GPa (10,000,000 psi). Mix designs for four of the mixes used in the study are summarized in Table 1.

Table 1
Mix Designs — kg/m$^3$ (Kozul and Darwin 1997)

| Concrete Mix | *w/cm* | *w* | *c/s/fa* | sand | rock |
|---|---|---|---|---|---|
| HSC$^+$1 | 0.26 | 125 | 410/48/24 | 740 | 1110 |
| HSC$^+$2 | 0.26 | 125 | 410/48/24 | 890 | 990 |
| WSC$^{++}$1 | 0.50 | 164 | 327/0/0 | 760 | 1110 |
| WSC$^{++}$2 | 0.50 | 164 | 327/0/0 | 880 | 970 |

$^+$High-strength concrete; $^{++}$Normal-strength concrete; *w/cm* = Water cementitious material ratio; *w* = water; *c* = portland cement; *s* = silica fume; *fa* = fly ash.

All material tests used the same basic specimen, a concrete prism with dimensions 100 x 100 x 355 mm (4 x 4 x 14 in.). Compressive tests were carried out by removing 25 mm (1 in.) from either end of the specimen, providing a ratio of height to width of 3 to 1. This minimizes the effect of end restraint, placing the center portion of the specimen under nearly uniaxial compression. The flexure and fracture specimens were tested under center point loading using a 305 mm (12 in.) span. The fracture specimen is shown in Figure 8. The test is similar to a flexure test, except that the specimen is notched at center span and the full load-deflection curve is measured. The test is run in a closed-loop testing machine and controlled with a clip gage that monitors the opening of the notch, called the *crack mouth opening displacement.*

While compressive and flexure tests are well known, only in recent years have the fracture properties of concrete received attention from structural engineers. Figure 9 shows a schematic of a load-deflection curve for a fracture specimen. The heavy line represents the measured curve. The area under the heavy curve is equal to the energy $W_0$. Since the principal goal of the fracture test is to determine the total energy dissipated during crack formation $W$, the energy due to the self weight of the specimen and any portion of the load system that is placed on the specimen prior to measuring deflection $W_1$ must be accounted for. In addition, the energy that would have been dissipated had the specimen been fully weight compensated $W_2$ must also be estimated. The total energy dissipated in crack formation can be represented as

$$W = W_o + W_1 + W_2 \qquad (1)$$

$W_1$ is the product of the weight of one-half of the specimen plus the weight of the load system that is placed on the specimen (represented as $mg/2$) and the maximum deflection measured during the test $\delta_f$. It can be shown that $W_2 \cong W_1$. Thus,

$$W = W_o + mg\delta_f \qquad (2)$$

Fracture energy, $G_f$, is equal to the total dissipated energy divided by the fractured area of the concrete $A$ (Figure 8).

$$G_f = (W_o + mg\delta_f)/A \qquad (3)$$

## Results and Evaluation

### *Compressive Strength*

The effect of aggregate type on the compressive strength of the four mixes in Table 1 is illustrated in Table 2.

Table 2
Compressive Strength as a Function of
Aggregate Type — Representative Results (Kozul and Darwin 1997)

| Concrete Mix | Basalt | Limestone |
|---|---|---|
| HSC⁺1 | 86 MPa | 75 MPa |
| HSC⁺2 | 78 MPa | 71 MPa |
| NSC⁺⁺1 | 28 MPa | 31 MPa |
| NSC⁺⁺2 | 25 MPa | 29 MPa |

⁺High-strength concrete; ⁺⁺Normal-strength concrete

The results indicate that, for high-strength concretes, the basalt coarse aggregate provides higher compressive strengths than does the limestone coarse aggregate at the same *w/cm* ratio. For example, for mix HSC 1, the concrete containing basalt had a compressive strength of 86 MPa (12,500 psi) compared to the limestone with a compressive strength of 75 MPa (11,900 psi). Other than the type of coarse aggregate, the mixes were the same. In contrast, for the normal-strength concretes, the limestone produced the same or slightly higher strengths. For mix NSC 1, basalt produced a compressive strength of 28 MPa (4,100 psi) compared to the limestone with a compressive strength of 31 MPa (4,500 psi).

***Flexural Strength***

Flexural strengths were consistently higher for concrete containing basalt, but generally flexural strengths were a function of compressive strength, as shown in Figure 10. The figure includes a curve representing the relationship between $f_c'$ and flexural strength defined in ACI 318-99, a relationship in which the flexural strength is proportional to $\sqrt{f_c'}$. It can be seen that the actual flexural strengths are higher than the curve and that the relationship between flexural strength and $f_c'$ is close to linear for these results.

***Fracture Energy***

Figures 11 and 12 show load-deflection curves for four tests. Figure 11 shows load-deflection curves for two normal-strength concretes, one containing basalt and one containing limestone. Although the maximum load, corresponding to the peak tensile stress in the tests, is nearly identical for the two concretes, the concrete containing the basalt dissipates significantly more energy, as represented by the area under the curves. Figure 12 shows the load-deflection curves for a high-strength and a low-strength concrete, both containing basalt. While the peak load carried by the high-strength concrete is nearly 60% higher than the peak load carried by the normal-strength concrete, the areas under the curves are nearly identical, indicating that they both have similar energy dissipation capacities.

Results from the fracture energy tests are summarized in Figure 13, which compares fracture energy to compressive strength for different mixes containing basalt and limestone coarse aggregate. In contrast to compressive and flexural strengths, fracture energy $G_f$ is not a function of the *w/cm* ratio or even age (the specimens in this figure range in age from 5 to 164 days), but rather of aggregate type. The fracture energy of the concrete containing the basalt coarse aggregate is approximately 2½ times that of the specimens containing the limestone coarse aggregate. For the concretes containing limestone, fracture energy increases slightly as compressive strength increases. For basalt, fracture energy decreases as compressive strength increases. The greater fracture energy of the concrete containing basalt helps explain the higher splice strength of the test specimens containing basalt coarse aggregate.

In all cases, the failure surfaces of the concretes containing basalt were rougher than those containing limestone. A rougher surface translates into a greater total fracture area and an increase in the energy required to form a crack (although surface roughness alone does not determine fracture energy).

Of special interest in the test results is the relationship between the peak calculated tensile stress in the fracture test with the flexural strength for the same concretes. The results are summarized in Figure 14. As can be seen in the figure, the relationship between these two measures of tensile strength is nearly linear, indicating that the maximum stress that can be attained at the tip of a crack will increase as a function of the compressive strength since flexural strength and compressive strength are closely related (Figure 10). The ramifications for structural behavior are important, since an increase in strength results in an increase in the tensile energy that can be stored just before a crack begins to propagate.

This point is emphasized by Figure 12, in which the load-deflection curves for high-strength and normal-strength fracture specimens are compared. As the compressive strength of concrete increases, its ability to sustain a tensile stress increases. But once the peak tensile stress is reached, the concrete possesses little more, and perhaps less, energy dissipation capacity to slow the propagation of the crack (Figure 13). The result is that high-strength concretes are more brittle than normal-strength concretes. In terms of structural design, the ability of concrete to *sustain* tensile stresses is significantly reduced compared to what might be expected based on compressive strength. Once a crack starts to move within the material, the extra energy, represented by the higher peak on the load-deflection curve, must be dissipated. Since a higher energy dissipation capacity is not available, commensurate with the increase in total energy stored, the structural strength of the member will be reduced. This is the principal reason for the low rate of increased bond strength as a function of compressive strength. While the tensile strength itself increases, the ability to prevent cracks from propagating rapidly decreases as concrete compressive strength improves. In a similar manner, the relatively poor response of the high-strength concrete shear specimens, observed by Collins and Kuchma (1999), can be explained by the same phenomenon.

The increasingly brittle tensile behavior of concrete as compressive strength increases indicates that high-strength concrete needs special attention during design for load cases in which tensile strength plays an important role. The two examples given in this paper are bond and shear strength. Thus, the addition of fibers and/or transverse reinforcement, to confine the concrete and increase its ductility, becomes increasingly important as concrete strength increases. The brittle nature of the compressive failure of high-strength concrete also supports the need for careful attention to transverse reinforcement for high-strength concrete columns.

## CONCLUSIONS

The principal conclusions from the observations reported are as follows:

1. Higher strength/higher stiffness aggregates provide higher compressive strengths for high-strength concrete, but lower compressive strengths for normal-strength concrete, compared to aggregates with lower strength and stiffness.

2. High-strength aggregates produce higher tensile strengths in both high and normal-strength concrete.

3. The fracture energy of concrete is governed principally by the aggregate properties, with higher strength aggregates producing concretes with higher fracture energies.

4. The fracture energy of concrete is generally independent of compressive strength, water-cementitious material ratio, or age.

5. Overall, as compressive strength of concrete increases, the energy stored in the material at the peak tensile load increases, while the ability of the material to dissipate energy remains approximately constant. The result is increasingly brittle behavior as compressive strength increases.

## IMPLICATIONS

The principal implication of the fracture behavior of high-strength concrete comes directly from the final conclusion. The increase in stored energy just before a crack begins to propagate, with no increase in ability to dissipate the energy stored in the material, means that the likelihood of brittle failures in high-strength concrete is greatly increased under conditions in which the tensile properties of the concrete govern structural behavior. To attain ductile behavior, those properties must be enhanced through the use of either fibers or additional reinforcing steel. It will, therefore, become increasingly important for the structural community to develop strategies to limit the probability of brittle failures in high-strength concrete structures and to ensure that designers are aware of the problems associated with high-strength concretes, as the compressive strengths used in practice continue to increase.

## ACKNOWLEDGEMENTS

This paper is based on research at the University of Kansas undertaken with support of the U. S. National Science Foundation under Research Grant No. CMS-9402563 and the U. S. Department of Transportation Federal Highway Administration. The research was carried out by the author, graduate students Rozalija Kozul, Shawn Barham, and visiting scholar Shuguang Luan of the Dalian Fisheries College, People's Republic of China.

## REFERENCES


ACI Committee 318. (1999). *Building Code Requirements for Structural Concrete (318-99)*, American Concrete Institute, Farmington Hills, Mich., U.S.A.

Ahmad, S. H. and Shah, S. P. (1985). "Standard Properties of High Strength Concrete and Its Implications for Precast Prestressed Concrete," *PCI Journal*, Vol. 30, No. 6, Nov.-Dec., pp. 92-119.

ASTM A 944-95. (1996). "Standard Test Method for Comparing Bond Strength of Steel Reinforcing Bars to Concrete Using Beam-End Specimens," American Society for Testing and Materials, West Conshohocken, Pennsylvania.

Barham, S. and Darwin, D. (1999). "Effects of Aggregate Type, Water-to-Cementitious Material Ratio, and Age on Mechanical and Fracture Properties of Concrete," *SM Report* No. 56, University of Kansas Center for Research, Inc., Lawrence, Kansas.

Brown, C. J., Darwin, D., and McCabe, S. L. (1993). "Finite Element Fracture Analysis of Steel-Concrete Bond," *SM Report* No. 36, University of Kansas Center for Research, Inc., Lawrence, Kansas.

Collins, M. P., and Kuchma, D. (1999). "How Safe Are Our Large, Lightly Reinforced Concrete Beams, Slabs, and Footings?" *ACI Structural Journal*, Vol. 96, No. 4, July-August, pp. 482-490.

Kozul, R. and Darwin, D. (1997). "Effects of Aggregate Type, Size, and Content on Concrete Strength and Fracture Energy," *SM Report* No. 43, University of Kansas Center for Research, Inc., Lawrence, Kansas.

Tholen, M. L. and Darwin, D.(1996) "Effects of Deformation Properties on the Bond of Reinforcing Bars," *SM Report* No. 42, University of Kansas Center for Research, Inc., Lawrence, Kansas.

Zuo, J. and Darwin, D. (1998). "Bond Strength of High Relative Rib Area Reinforcing Bars," *SM Report* No. 46, University of Kansas Center for Research, Inc., Lawrence, Kansas.

Zuo, J. and Darwin, D. (2000). "Bond Slip of High Relative Rib Area Bars under Cyclic Loading," *ACI Structural Journal*, Vol. 97, No. 2, Mar. - Apr., pp. 331-334.

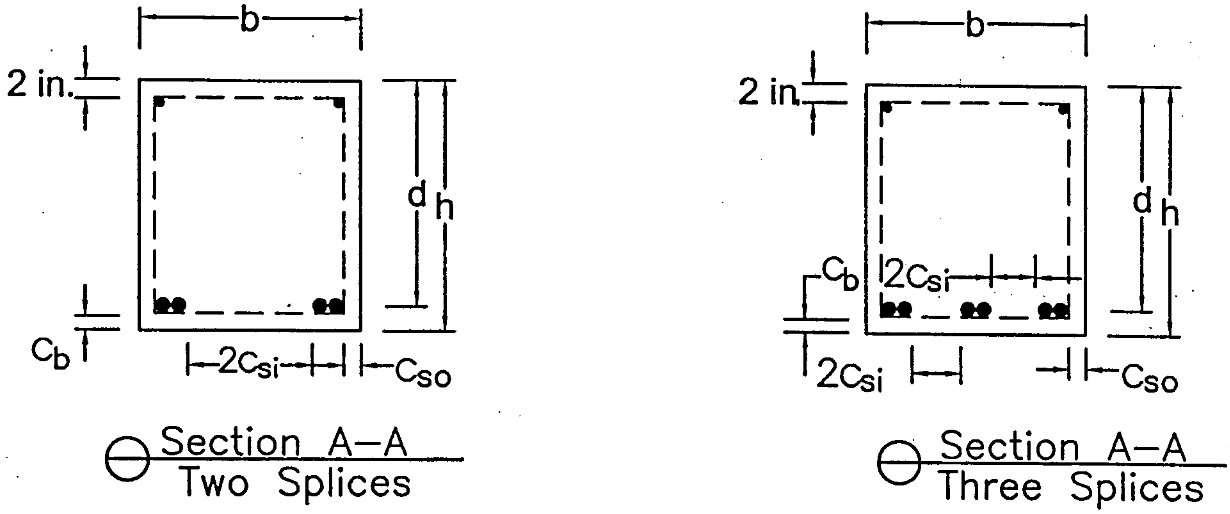


Figure 1 Cross sections of typical splice specimens (Zuo and Darwin 2000)

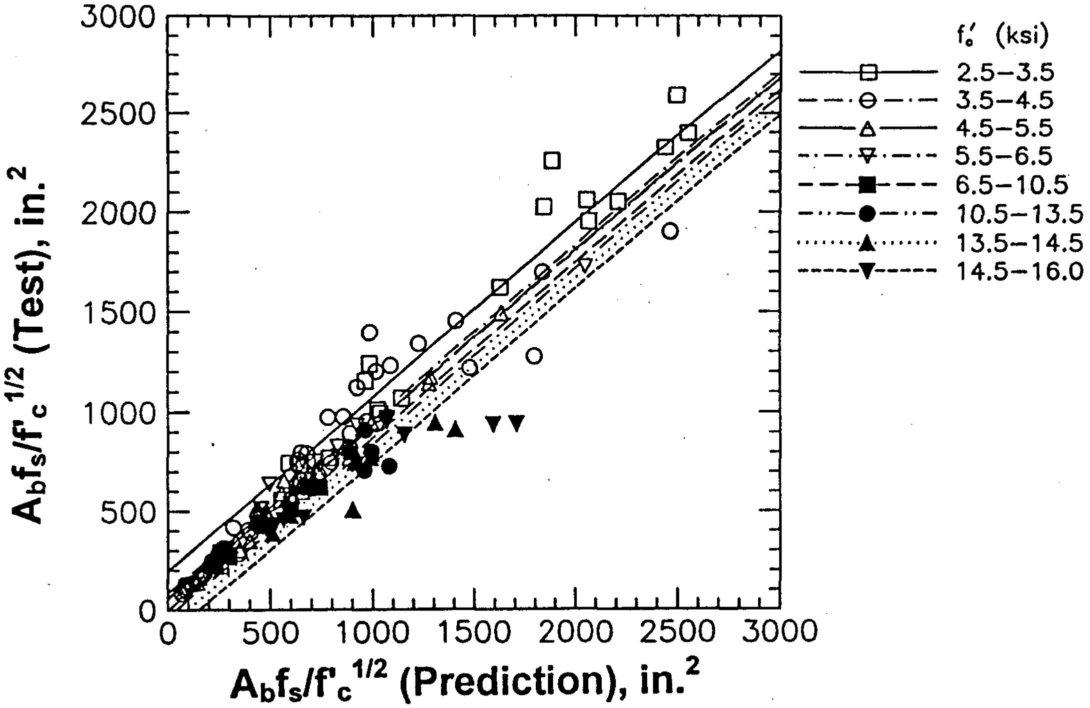


Figure 2 Comparison between test and predicted strengths for splice tests in which concrete strength is characterized by $f_c'^{1/2}$(after Zuo and Darwin 1998)

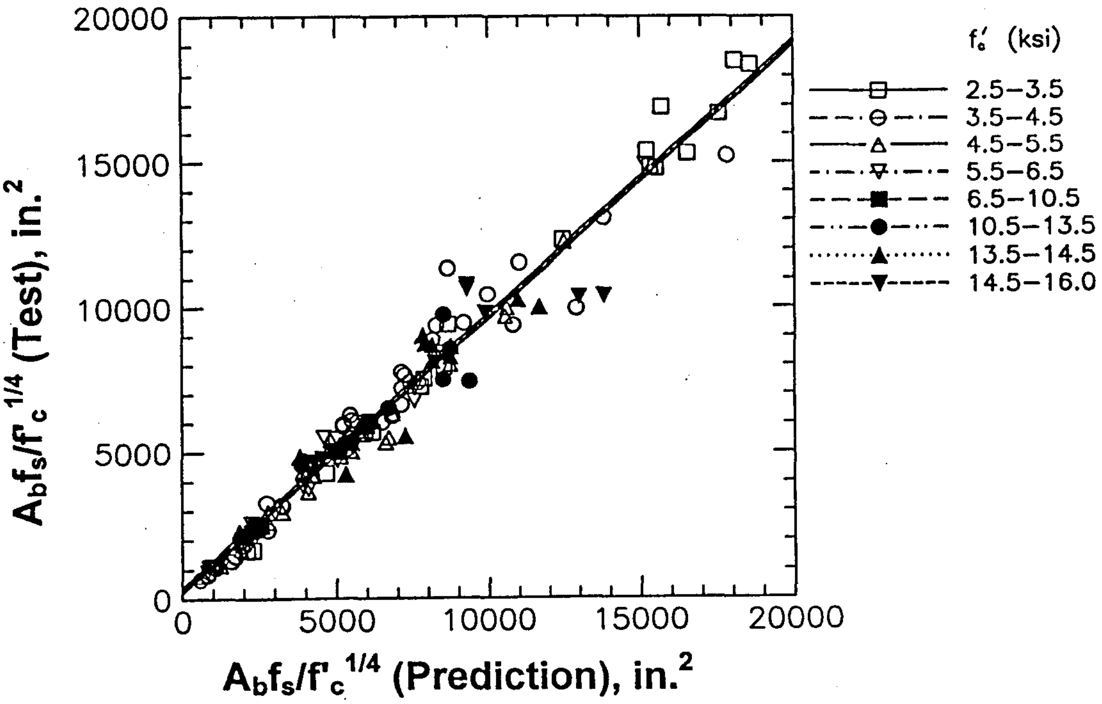


Figure 3 Comparison between test and predicted strengths for splice tests in which concrete strength is characterized by $f_c'^{1/4}$( after Zuo and Darwin 1998)

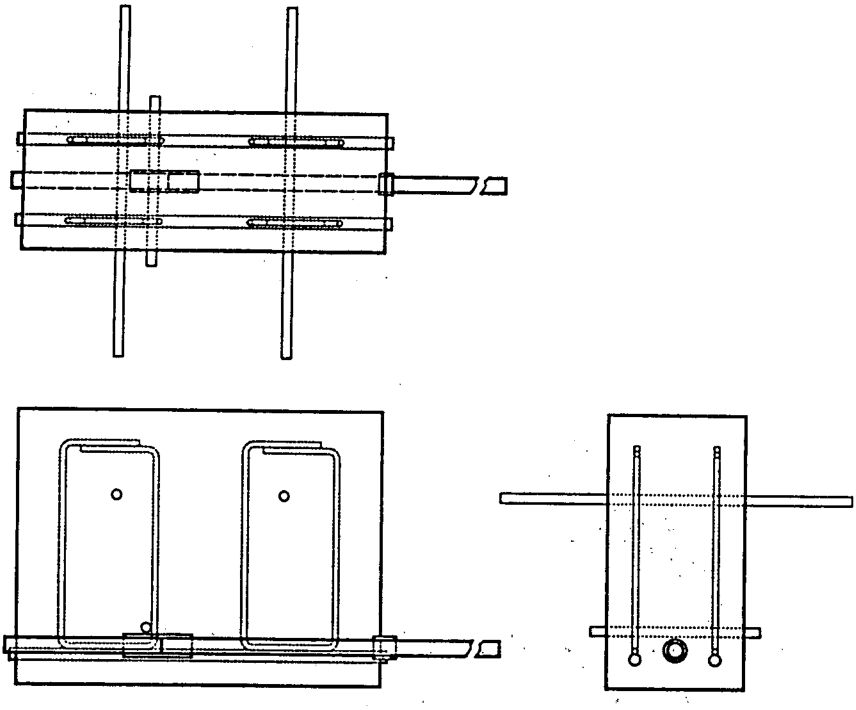

(a)

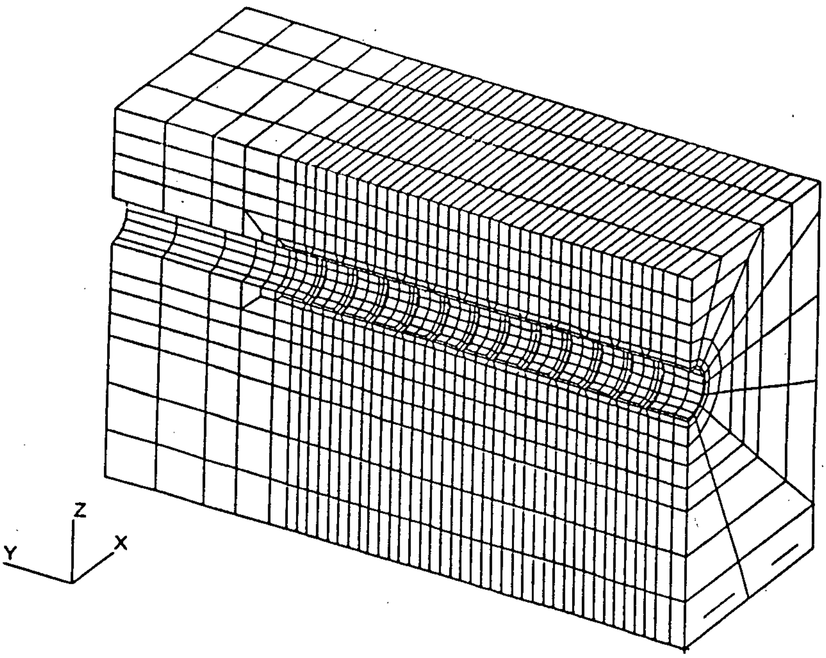


(b)

Figure 4 Beam-end specimen (a) test specimen, (b) finite element representation (Tholen and Darwin 1996)

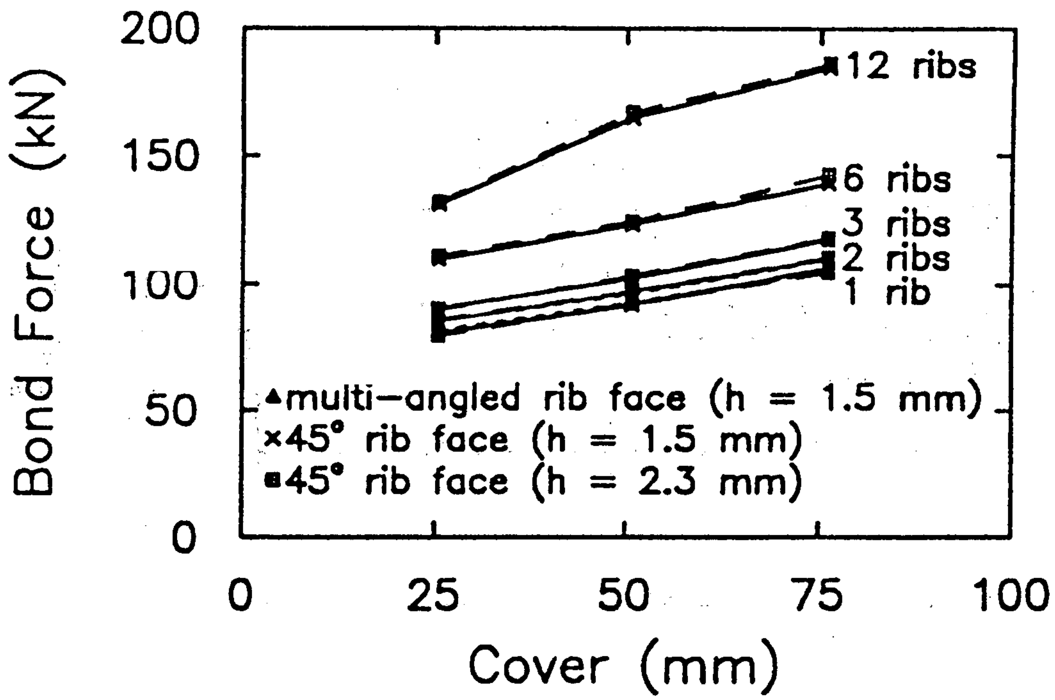


Figure 5 Bond force versus cover and development length for finite element model of beam-end specimen (Brown, Darwin and McCabe 1993)

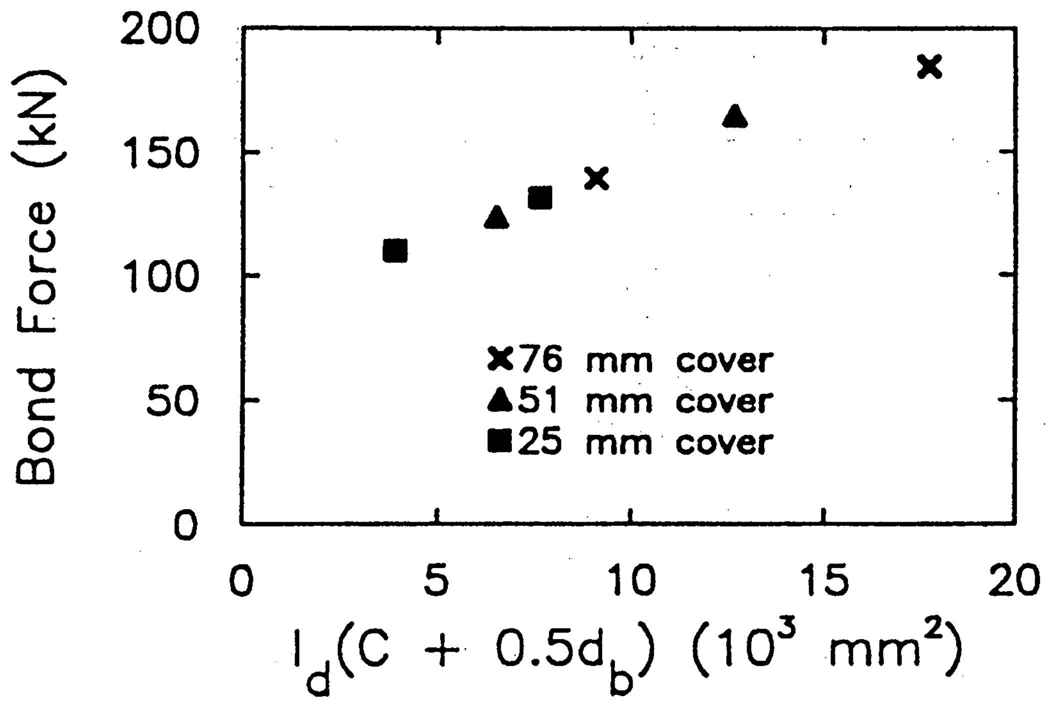


Figure 6 Bond force versus product of development length and cover to the center of the bar for finite element model of beam-end specimen (Brown, Darwin and McCabe 1993)

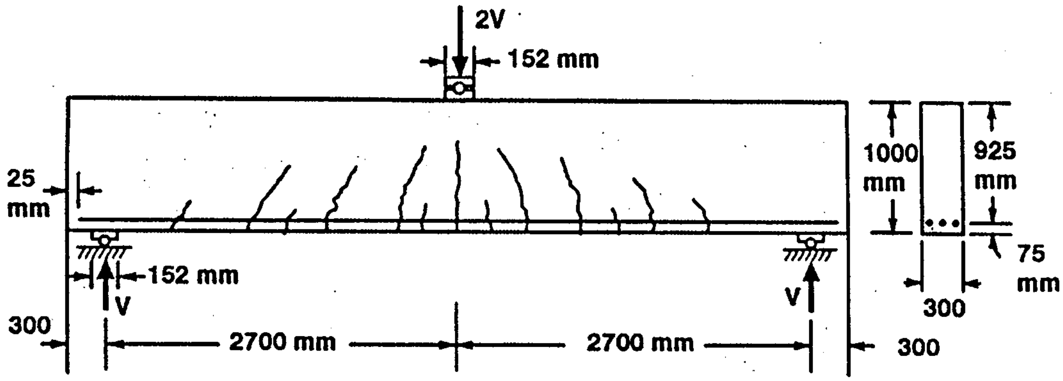


Figure 7 Full-scale shear test specimen (Collins and Kuchma 1999)

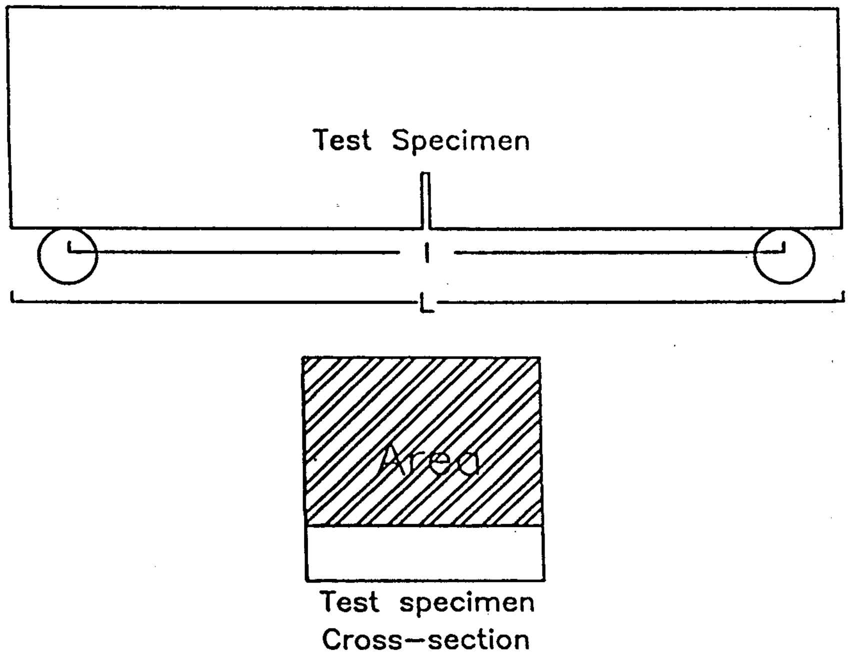


Figure 8 Schematic of fracture specimen (Kozul and Darwin 1997)

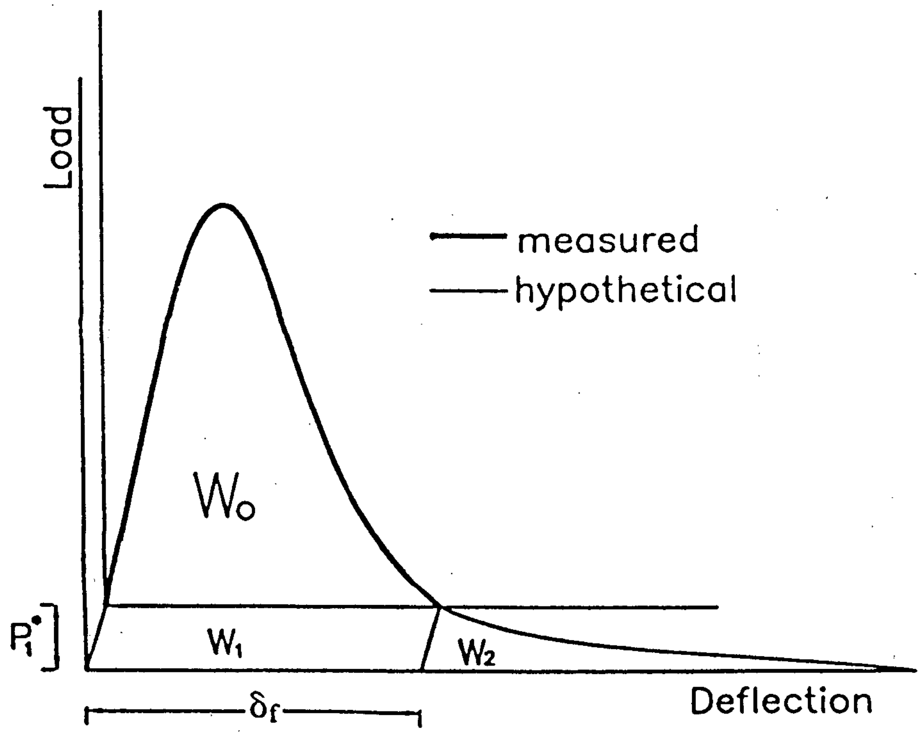


Figure 9 Schematic of load-deflection curve for fracture energy test specimen (Kozul and Darwin 1997)

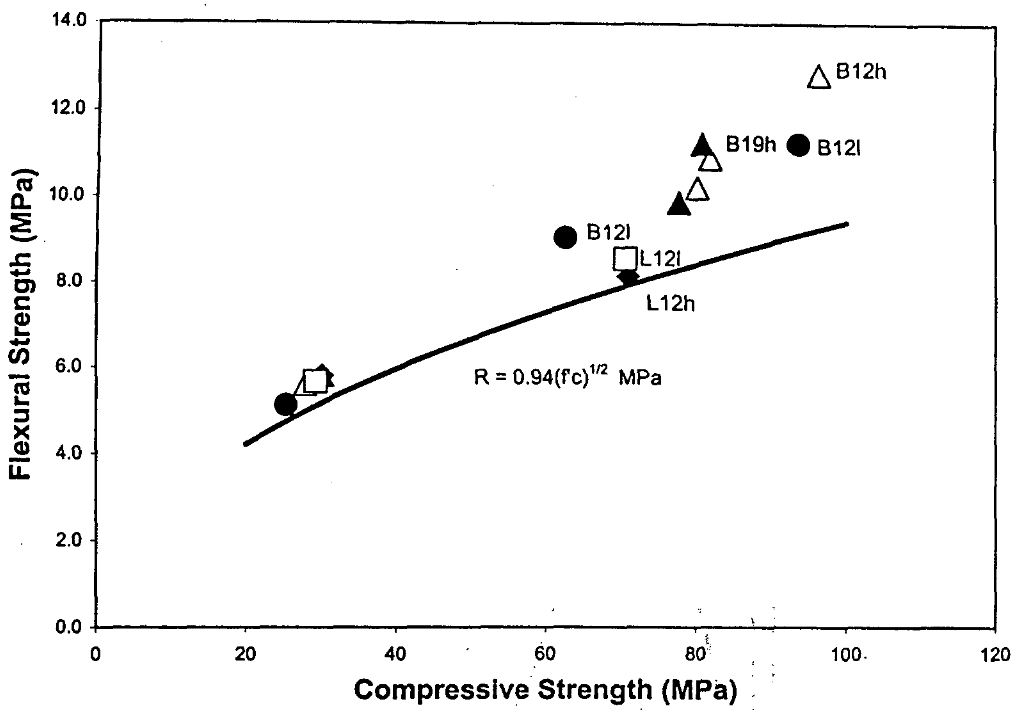


Figure 10 Flexural strength versus compressive strength for normal and high-strength concretes. B = basalt; L = limestone; R = flexural strength (Kozul and Darwin 1997)

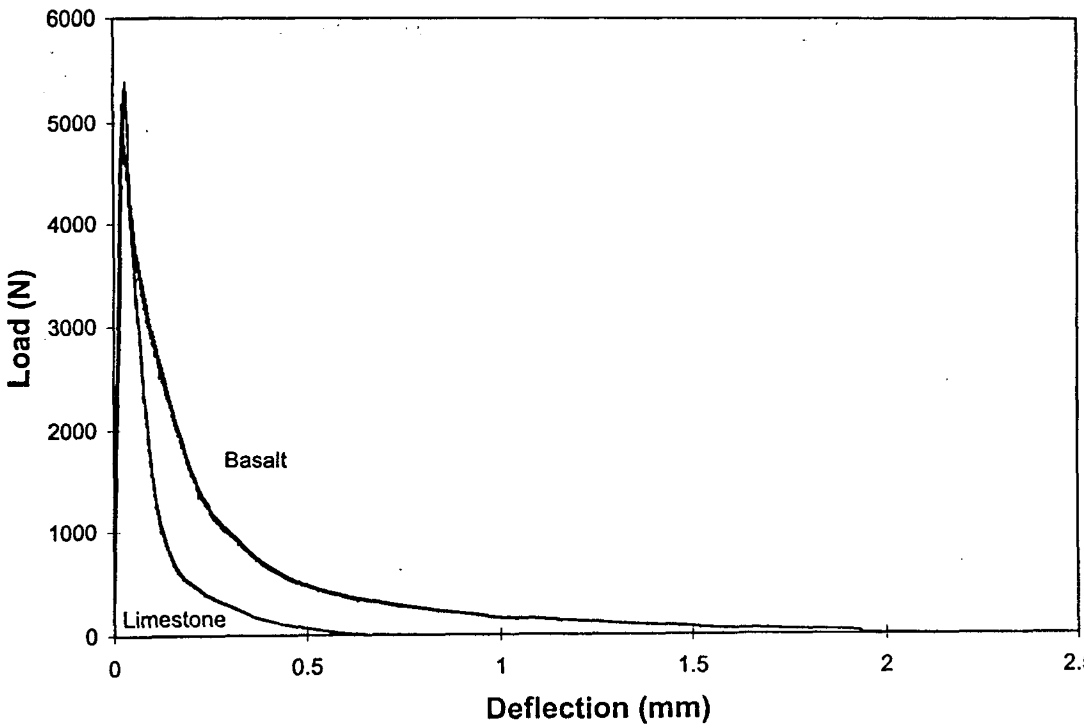


Figure 11 Load-deflection curves for normal-strength concretes containing basalt and limestone (Kozul and Darwin 1997)

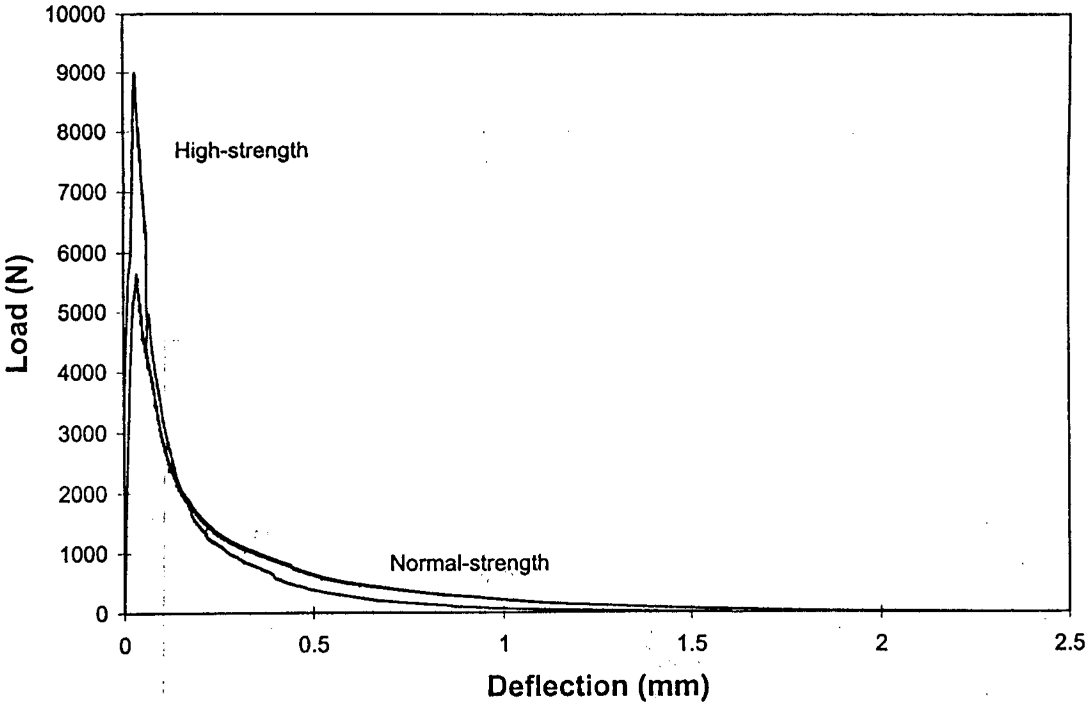


Figure 12 Load-deflection curves for high-strength and normal-strength concretes containing basalt (Kozul and Darwin 1997)

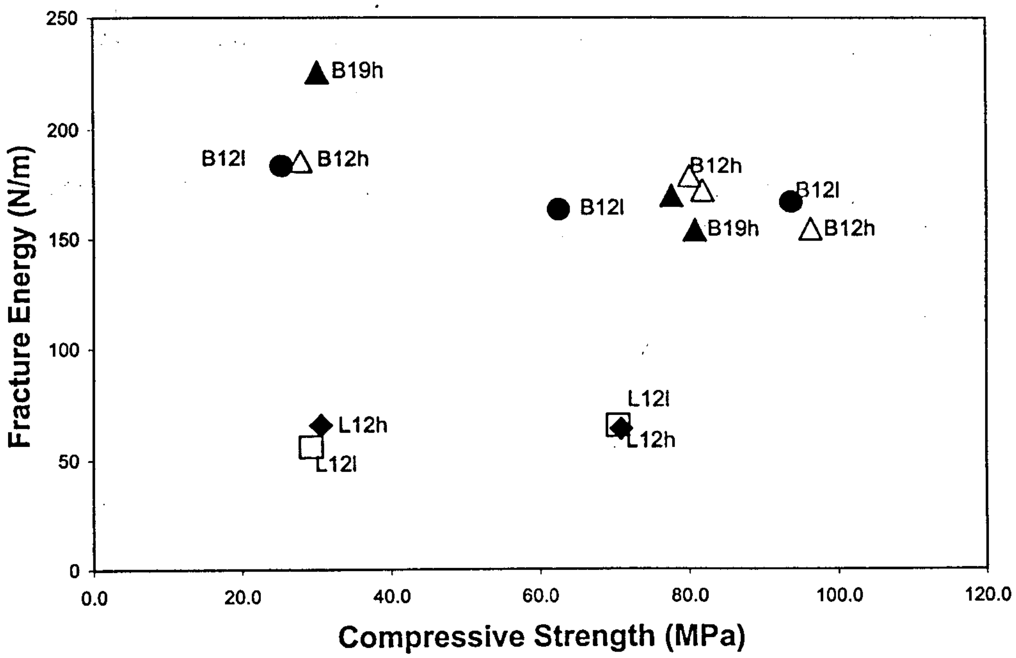


Figure 13 Fracture energy versus compressive strength for concretes containing limestone and basalt coarse aggregates (Kozul and Darwin 1997)

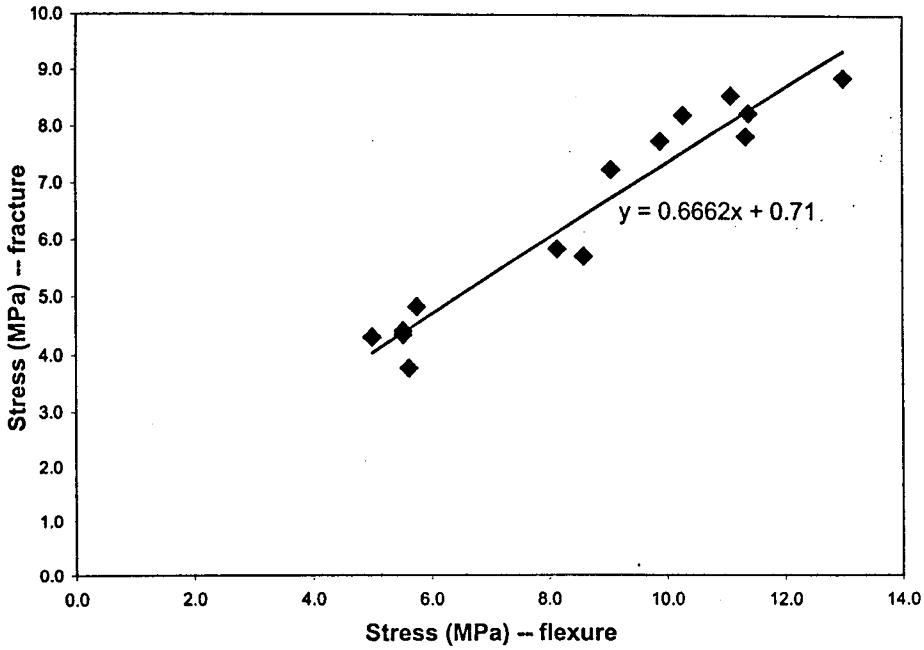


Figure 14 Relationship between the peak tensile stress in fracture tests and flexural strength for normal and high-strength concretes containing basalt and limestone coarse aggregates (Kozul and Darwin 1997).